An Accurate Deterministic Projection Method for Two-Dimensional Stiff Detonation Waves

Alina Chertock*, Shaoshuai Chu†, and Alexander Kurganov‡

Abstract

We extend the accurate deterministic projection method, which was introduced as a simple underresolved method for one-dimensional hyperbolic systems with stiff source term, to two-dimensional reactive Euler equations of gas dynamics. In addition to shock, contact and rarefaction waves, these equations admit detonation waves appearing at the interface between the burnt and unburnt fractions of the gas. In order to resolve the reaction zone numerically, one has to take both space and time stepsizes to be proportional to the reaction time, which may be very computationally expensive or even practically impossible when the reaction is fast. Therefore, it is necessary to develop underresolved numerical methods, which are capable of accurately predicting locations of the detonation waves without resolving their detailed structure. We propose such method for the case of stiff detonation waves and demonstrate the robustness of this method on a number of numerical experiments.

Key words: stiff detonation waves, reactive Euler equations, splitting method, deterministic projection method, central-upwind scheme.
AMS subject classification: 76M12, 65M08, 76V05, 35L65, 35L67.

1 Introduction

We study numerical methods for two-dimensional (2-D) hyperbolic systems of balance laws with very stiff source terms:

$$\boldsymbol{U}_t + \boldsymbol{F}(\boldsymbol{U})_x + \boldsymbol{G}(U)_y = \frac{1}{\varepsilon}\boldsymbol{S}(\boldsymbol{U}), \quad 0 < \varepsilon \ll 1, \tag{1.1}$$

where, $\boldsymbol{U}$ is an unknown function of space variables x and y and a time variable t, $\boldsymbol{F}$ and $\boldsymbol{G}$ are given flux functions and $\boldsymbol{S}$ is a source term. In particular, we consider an inviscid, compressible,

---

*Department of Mathematics, North Carolina State University, Raleigh, NC 27695, USA; chertock@math.ncsu.edu

†Department of Mathematics, Southern University of Science and Technology, Shenzhen, 518055, China; 11930702@mail.sustech.edu.cn

‡Department of Mathematics and SUSTech International Center for Mathematics, Southern University of Science and Technology, Shenzhen, 518055, China; alexander@sustech.edu.cn

reacting flow, governed by the reactive Euler equations:

$$
\begin{pmatrix} \rho \\ \rho u \\ \rho v \\ E \\ \rho z \end{pmatrix}_t + \begin{pmatrix} \rho u \\ \rho u^2 + p \\ \rho uv \\ u(E+p) \\ \rho uz \end{pmatrix}_x + \begin{pmatrix} \rho v \\ \rho uv \\ \rho v^2 + p \\ v(E+p) \\ \rho vz \end{pmatrix}_y = \frac{1}{\varepsilon} \begin{pmatrix} 0 \\ 0 \\ 0 \\ 0 \\ -\rho z K(\tau) \end{pmatrix}.
\tag{1.2}
$$

Here, the dependent variables ρ, u, v, E and z are the density, x- and y-velocities, total energy and the fraction of unburnt gas, respectively. The system is completed through the following equation of state (EOS):

$$
p = (\gamma - 1)\left[E - \frac{\rho}{2}(u^2 + v^2) - q_0\rho z\right],
\tag{1.3}
$$

where the parameters γ and q_0 represent the specific heat ratio and chemical heat release, respectively. On the right-hand side (RHS) of (1.2), $\tau := p/\rho$ is the temperature and ε is the reaction time. Finally, the Arrhenius kinetic term is

$$
K(\tau) = e^{-\tau_c/\tau},
\tag{1.4}
$$

where τ_c is the ignition temperature.

We are interested in regimes of fast detonation waves, when chemical reaction time scales are much faster than the fluid dynamical ones. Therefore, in order to fully (numerically) resolve detonation waves, one has to take both temporal (Δt) and spatial ($\Delta x, \Delta y$) grid scales to be proportional to ε. This may be extremely computationally expensive, even practically impossible. This is the major reason why one may be interested in developing *underresolved* numerical methods, in which $\Delta t, \Delta x, \Delta y \gg \varepsilon$. In such a case, the chemical reaction may be considered infinitely fast and thus the Arrhenius kinetics term (1.4) may be replaced with (even stiffer) Heaviside kinetics term [33]:

$$
K(\tau) = H(\tau - \tau_c) = \begin{cases} 1, & \text{if } \tau \geq \tau_c, \\ 0, & \text{otherwise.} \end{cases}
\tag{1.5}
$$

The difference in the kinetics affects the details of the detonation layers, which are of width $\mathcal{O}(\varepsilon)$ with the pressure and temperature spikes that decay exponentially into the postdetonation equilibria.

Designing an accurate underresolved numerical method for the very stiff system (1.2), (1.3), (1.5), or, in general, for the system (1.1) with a very small ε, is a rather challenging problem. Since the system is stiff, it is natural that one may wish to use an operator splitting (fractional step) method; see, e.g., [26, 27]. The latter can be implemented by considering the following two subsystems:

$$
\boldsymbol{U}_t + \boldsymbol{F}(\boldsymbol{U})_x + \boldsymbol{G}(\boldsymbol{U})_y = \boldsymbol{0}
\tag{1.6}
$$

and

$$
\boldsymbol{U}_t = \frac{1}{\varepsilon}\boldsymbol{S}(\boldsymbol{U}).
\tag{1.7}
$$

Then, assuming that $\boldsymbol{U}(x,t)$ is available at time t, an approximate solution at the next time level $t + \Delta t$ is given by

$$
\boldsymbol{U}(x,y,t+\Delta t) = S_{\mathcal{P}}(\Delta t)S_{\mathcal{H}}(\Delta t)\boldsymbol{U}(x,y,t),
$$

where $S_\mathcal{P}$ and $S_\mathcal{H}$ denote the solution operators for the subsystems (1.6) and (1.7), respectively. In the case under consideration, the step of solving the ODE (1.7) reduces to the projection of the computed solution onto an equilibrium state:

$$\boldsymbol{U} \mapsto \mathcal{P}\boldsymbol{U}, \tag{1.8}$$

where $\boldsymbol{S}(\mathcal{P}\boldsymbol{U}) \equiv \boldsymbol{0}$, while the corresponding hyperbolic system of conservation laws (1.6) can be solved by any (stable and sufficiently accurate) shock-capturing method. In this paper, we use the second-order central-upwind scheme briefly described in Appendix A. Central-upwind schemes are Riemann-problem-solver-free Godunov-type schemes for general multidimensional hyperbolic systems of conservation laws. These schemes were first proposed in [23] and then further developed in [20–22, 24].

Even though the operator splitting method is very simple, it has a major drawback: If the deterministic projection operator is used in (1.8), this approach may lead to a spurious weak detonation wave that travels with a nonphysical propagation speed. This occurs since shock-capturing methods smear discontinuities, and as soon as the nonphysical value of the temperature in this numerical layer is above the ignition temperature, a certain part of the gas may get numerically burnt prematurely. This peculiar numerical phenomenon was first observed in [9, 10], and since then it has attracted lots of attention; see, e.g. [3, 4, 6, 14, 25, 29]. In order to fix this numerical problem, the ignition temperature was artificially increased in [5], or replaced with uniformly distributed random variable; see, e.g., random projection, [1, 2], or random choice, [8], method. Numerical methods using overlapping grids and block-structured adaptive mesh refinement for high-speed reactive flow in complex geometries were proposed in [16, 17]. Other, more complicated, but rather successful approaches have been proposed in [7, 11, 15, 32, 34].

A simple and robust alternative to the aforementioned approaches was proposed in [19], where an accurate deterministic projection (ADP) method for one-dimensional (1-D) hyperbolic systems with stiff source terms was introduced. The key idea of the ADP method is to evolve $\boldsymbol{U}$ according to the homogeneous system (1.6) (this guarantees the correct propagation speed), while using the projected values of $\tilde{\boldsymbol{U}} := \mathcal{P}\boldsymbol{U}$ only whenever they required (for example, for computing the pressure values using the EOS when the reactive Euler system is considered).

In this paper, we extend the ADP method to the 2-D reactive Euler equations (1.2), (1.3), (1.5). The paper is organized as follows. In §2, we describe the "standard" deterministic projection method, which is known to generate artificial waves propagating with non-physical speeds. In §3, we propose a very simple correction and introduce the ADP method for the 2-D reactive Euler equations. The resulting method is tested in §4 on four numerical examples. We study the propagation of a detonation wave in a channel, radial detonation wave, interaction of multiple gas dynamics waves with a detonation wave, and the diffraction of a detonation wave around a solid corner. In all of the examples, the proposed ADP method is sufficiently accurate (being an underresolved method, the ADP method cannot capture detonation waves in detail, but it is capable of accurately predicting the position of the wave) and robust. We provide some concluding remarks and ventures for the future work in §5.

2 "Standard" Deterministic Projection Method

In this section, we describe a "standard" deterministic projection approach for solving the reactive Euler equations (1.2), (1.3), (1.5). For simplicity, we consider a rectangular computational

domain covered by a uniform spatial mesh consisting of the cells $C_{j,k}$ centered at $(x_j, y_k) :=$ $(j\Delta x, k\Delta y)$ and assume that the computed solution is realized in terms of its cell averages, $\overline{U}^n_{j,k} = \frac{1}{\Delta x \Delta y} \int_{C_{j,k}} U(x, y, t^n)$ and available at time level $t = t^n$. In order to evolve the solution to the next time level according to the aforementioned operator splitting approach, we first use a (stable and accurate) shock-capturing method to numerically solve the homogeneous system

$$
\begin{pmatrix} \rho \\ \rho u \\ \rho v \\ E \\ \rho z \end{pmatrix}_t + \begin{pmatrix} \rho u \\ \rho u^2 + p \\ \rho uv \\ u(E + p) \\ \rho uz \end{pmatrix}_x + \begin{pmatrix} \rho v \\ \rho uv \\ \rho v^2 + p \\ v(E + p) \\ \rho vz \end{pmatrix}_y = \begin{pmatrix} 0 \\ 0 \\ 0 \\ 0 \\ 0 \end{pmatrix},
\tag{2.1}
$$

completed through the EOS (1.3). Here, we prefer to work with finite-volume methods (in particular, with the central-upwind scheme described in Appendix A), but would like to stress that the considered computational framework is general and may be used in conjunction with one's favorite shock-capturing method. The cell averages $\overline{\rho}^{n+1}_{j,k}$, $(\overline{\rho u})^{n+1}_{j,k}$, $(\overline{\rho v})^{n+1}_{j,k}$, $\overline{E}^{n+1}_{j,k}$ and $(\overline{\rho z})^*_{j,k}$ at the new time level $t^{n+1} := t^n + \Delta t$ are then used to obtain $u^{n+1}_{j,k} = (\overline{\rho u})^{n+1}_{j,k} / \overline{\rho}^{n+1}_{j,k}$, $v^{n+1}_{j,k} = (\overline{\rho v})^{n+1}_{j,k} / \overline{\rho}^{n+1}_{j,k}$,

$$
p^{n+1}_{j,k} = (\gamma - 1) \left[\overline{E}^{n+1}_{j,k} - \frac{\overline{\rho}^{n+1}_{j,k}}{2} \left((u^{n+1}_{j,k})^2 + (v^{n+1}_{j,k})^2 \right) - q_0 (\overline{\rho z})^*_{j,k} \right],
\tag{2.2}
$$

and the corresponding temperature values,

$$
\tau^{n+1}_{j,k} = \frac{p^{n+1}_{j,k}}{\overline{\rho}^{n+1}_{j,k}}.
\tag{2.3}
$$

Notice that for the $(\overline{\rho z})^*_{j,k}$ quantities in (2.2), the upper index is not $n + 1$ yet as they are going to be changed after the following projection step, at which the values of z and ρz at time level $t = t^{n+1}$ are computed:

$$
z^{n+1}_{j,k} = \begin{cases} 0, & \text{if } \tau^{n+1}_{j,k} \geq \tau_c, \\ 1, & \text{if } \tau^{n+1}_{j,k} < \tau_c, \end{cases} \qquad (\overline{\rho z})^{n+1}_{j,k} = \overline{\rho}^{n+1}_{j,k} \cdot z^{n+1}_{j,k}.
$$

This "standard" deterministic projection method is very simple, but it may lead to spurious, nonphysical waves traveling with an artificial speed. Utilizing the ADP method presented in the next section allows one to avoid such an undesirable situation.

3   Accurate Deterministic Projection Method

The main reason of the failure of the "standard" deterministic projection method is that it uses nonphysical, artificial values of $(\overline{\rho z})^*_{j,k}$ obtained after the fluid dynamics step $S_{\mathcal{H}}$ of the operator splitting method. The simplest way to prevent this undesirable situation is not to solve the (ρz)-equation at the fluid dynamics step at all. We thus modify the deterministic projection method as follows.

Once again, we assume that cell averages of the solution at time level $t = t^n$ (including the values of the fraction of unburnt gas $z_{j,k}^n = (\overline{\rho z})_{j,k}^n / \overline{\rho}_{j,k}^n$) has been already computed. We first evolve it in time by applying a (stable and accurate) shock-capturing finite-volume method to the homogeneous system that contains only first four equations from the system (2.1):

$$
\begin{pmatrix} \rho \\ \rho u \\ \rho v \\ E \end{pmatrix}_t + \begin{pmatrix} \rho u \\ \rho u^2 + p \\ \rho uv \\ u(E + p) \end{pmatrix}_x + \begin{pmatrix} \rho v \\ \rho uv \\ \rho v^2 + p \\ v(E + p) \end{pmatrix}_y = \begin{pmatrix} 0 \\ 0 \\ 0 \\ 0 \end{pmatrix}, \tag{3.1}
$$

completed through the EOS (1.3). As before, the evolved cell averages $\overline{\rho}_{j,k}^{n+1}$, $(\overline{\rho u})_{j,k}^{n+1}$, $(\overline{\rho v})_{j,k}^{n+1}$ and $\overline{E}_{j,k}^{n+1}$ (but not $(\overline{\rho z})_{j,k}^*$, which is not computed now at all) are used to obtain $u_{j,k}^{n+1}$, $v_{j,k}^{n+1}$ and

$$
p_{j,k}^{n+1} = (\gamma - 1)\left[\overline{E}_{j,k}^{n+1} - \frac{\overline{\rho}_{j,k}^{n+1}}{2}\left((u_{j,k}^{n+1})^2 + (v_{j,k}^{n+1})^2 \right) - q_0\,\overline{\rho}_{j,k}^{n+1} \cdot z_{j,k}^n \right], \tag{3.2}
$$

Notice that compared with (2.2), the pressure in (3.2) is computed using the values of z from the previous time level, which is one of the crucial points in the ADP method.

The projection step is then performed as in the case of the "standard" deterministic projection method, namely, we set

$$
z_{j,k}^{n+1} = \begin{cases} 0, & \text{if } \tau_{j,k}^{n+1} \geq \tau_c, \\ 1, & \text{if } \tau_{j,k}^{n+1} < \tau_c, \end{cases}
$$

where the temperature values $\tau_{j,k}^{n+1}$ are obtained by (2.3).

4 Numerical Examples

In this section, we demonstrate the performance of the proposed ADP method and compare it with the "standard" deterministic projection (SDP) method. The fluid dynamics step is carried out using the second-order central-upwind scheme briefly described in Appendix A. In the first three examples, we take the CFL number 0.5 (the time step Δt is determined by using the CFL condition for the homogeneous systems (2.1) and (3.1)), while in the fourth one we use a smaller CFL number 0.25 to avoid small oscillations appearing when a larger time step is used.

Example 1—Detonation Wave in a Channel

We consider the initial-boundary value problem taken from [1]. The initial data,

$$
(\rho(x,y,0), u(x,y,0), v(x,y,0), p(x,y,0), z(x,y,0)) = \begin{cases} (\rho_l, u_l, 0, p_1, 0), & \text{if } x \leq \xi(y), \\ (\rho_r, u_r, 0, p_r, 1), & \text{if } x > \xi(y), \end{cases}
$$

where

$$
\xi(y) = \begin{cases} 0.004, & \text{if } |y - 0.0025| \geq 0.001, \\ 0.005 - |y - 0.0025|, & \text{if } |y - 0.0025| < 0.001, \end{cases}
$$

are given in a 2-D channel $[0, 0.025] \times [0, 0.005]$ with the solid wall boundary conditions at the upper and lower boundaries and free boundary conditions on the left and on the right. We take the following parameter values:

$$\gamma = 1.4, \quad q_0 = 0.5196 \times 10^{10}, \quad \frac{1}{\varepsilon} = 0.5825 \times 10^{10}, \quad \tau_c = 0.1155 \times 10^{10},$$

and the initial values: $\rho_l = 1.945 \times 10^{-3}$, $p_l = 6.27$, $u_l = 8.162$, $\rho_r = 1.201 \times 10^{-3}$, $p_r = 8.321$ and $u_r = 0$, which are the same as in [1].

One important feature of this solution is that the triple points travel in the transverse direction and bounce back and forth against the upper and lower walls, forming a cellular pattern.

We compute the solutions by using both the ADP and SDP methods on a uniform spatial mesh with $\Delta x = \Delta y = 5 \times 10^{-5}$. In Figure 4.1, we show the density computed at four different times using the ADP (top row) and SDP (bottom row) methods. The ADP results are in a good agreement with the results reported in [1], while the SDP solution develops a wave traveling with a non-physical speed. This can also be clearly seen in Figure 4.2, where we show the propagation of the interface between the burnt and unburnt fractions of the gas, computed by the two studied methods.
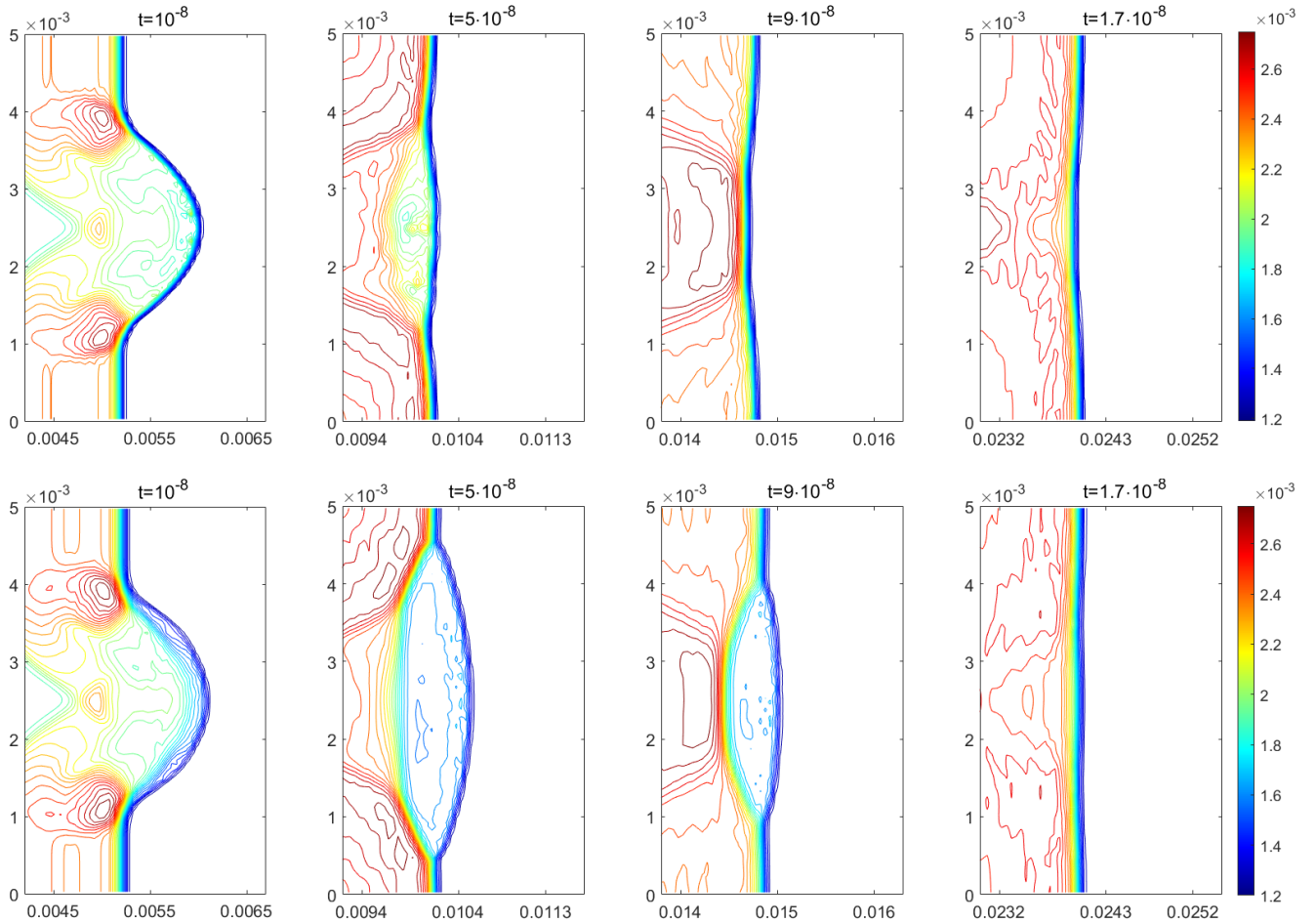
Figure 4.1: Example 1: Density ρ computed by the ADP (top row) and SDP (bottom row) methods.
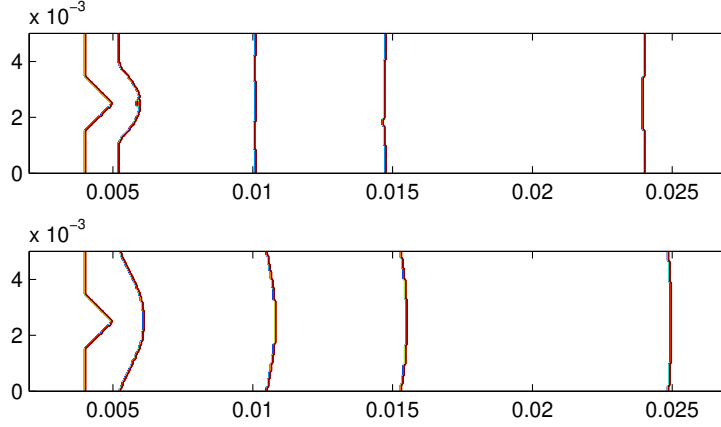
Figure 4.2: Example 1: Time evolution of the fraction of unburnt gas z computed by the ADP (top row) and SDP (bottom row) methods. In both figures, the detonation wave propagates from left to right and the interface between the burnt and unburnt fractions of the gas is shown at times $t = 0, 10^{-8}, 5 \cdot 10^{-8}, 9 \cdot 10^{-8}, 1.7 \cdot 10^{-7}$.

Example 2—Radial Detonation Wave

In the second example taken from [2], we consider the following radially symmetric initial data:

$$(\rho, u, v, p, z)(x, y, 0) = \begin{cases} (\rho_{\text{in}}, u_{\text{in}}(x, y), v_{\text{in}}(x, y), p_{\text{in}}, 0), & \text{if } r \le 10, \\ (1, 0, 0, 1, 1), & \text{if } r > 10, \end{cases} \quad r = \sqrt{x^2 + y^2},$$

where $p_{\text{in}} = 21.53134$, $\rho_{\text{in}} = 1.79463$, $u_{\text{in}}(x, y) = 10x/r$, and $v_{\text{in}}(x, y) = 10y/r$. The parameters are chosen as

$$\gamma = 1.2, \quad q_0 = 50, \quad \frac{1}{\varepsilon} = 1000, \quad \tau_c = 2.$$

The initial setting that consists of totally burnt gas inside a semi-circle with radius 10 and totally unburnt gas outside the semi-circle and the radially symmetric initial velocities corresponds to a circular detonation front.

We take the computational domain $[-50, 50] \times [0, 50]$ and use a uniform spatial mesh with $\Delta x = \Delta y = 1$. The solid wall boundary conditions are used along the bottom part of the domain, while the free boundary conditions are implemented at the other parts of the boundary. We have solved the problem numerically by both the ADP and SDP methods and the obtained results are reported in Figures 4.3–4.5.

In Figure 4.3, we show the density component of the computed solution at times $t = 0.25$, 1 and 3. As one can see, the difference in the density field captured by the ADP and SDP methods seems to be very small. However, the ADP and SDP temperatures, plotted in Figure 4.4, are totally different even at a smaller time $t = 0.25$. The source of this difference can be understood by looking at the propagation of the interface between the burnt and unburnt fractions of the gas shown in Figure 4.5. As the ADP solution is in a good agreement with the solution reported in [2], we conclude that the fast wave developed by the SDP solution is a numerical artifact that can be prevented by using the proposed accurate deterministic projection.
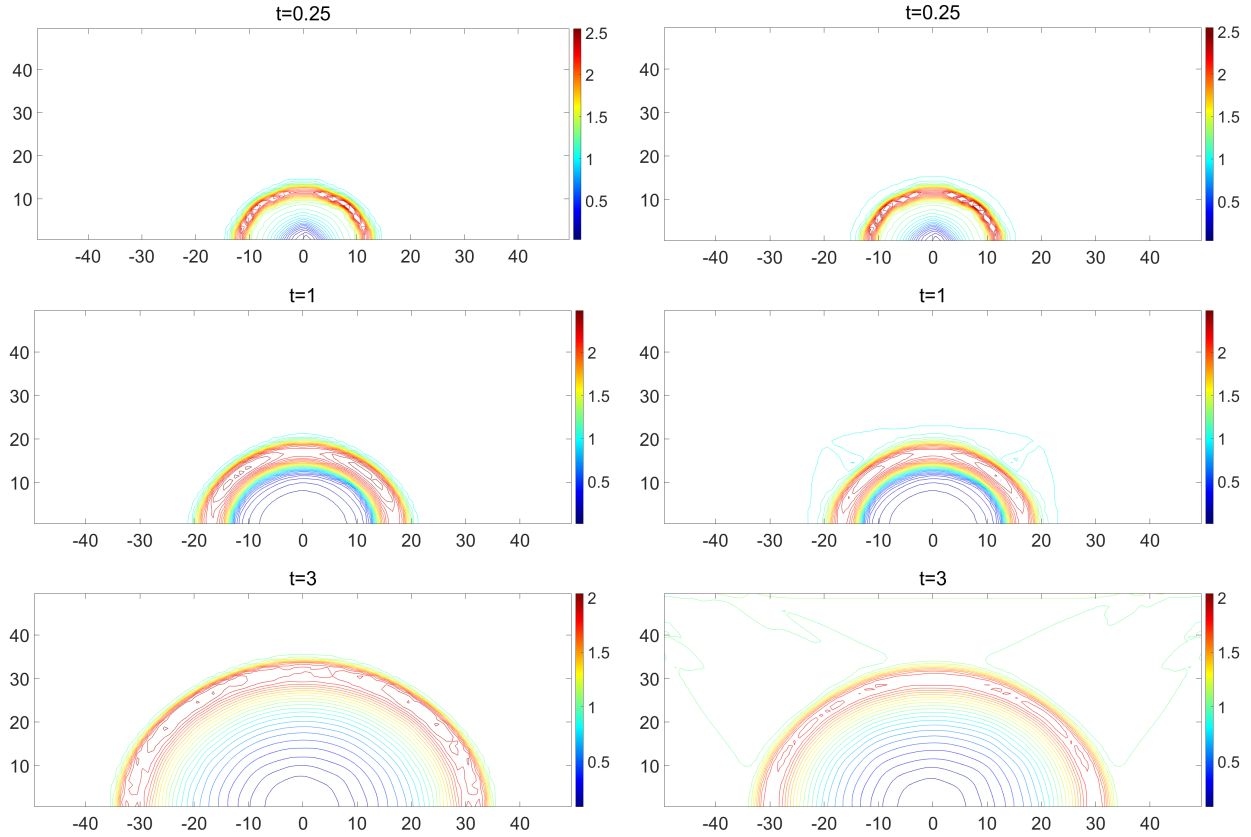
Figure 4.3: Example 2: Density ρ computed by the ADP (left column) and SDP (right column) methods.

Example 3—Interaction of Gas Dynamics and Detonation Waves

In the third example, we study the collision of a radially symmetric stiff detonation wave with a shock, contact discontinuity and rarefaction wave. This problem is an extension of the 1-D experiment conducted in [2, 18, 19]. We consider the following initial data:

$$(\rho, u, v, p, z)(x, y, 0) = \begin{cases} (4, 0, 0, 10, 0), & \text{if } x > 40, \\ (3.64282, 10\cos\theta, 10\sin\theta, 54.8244, 0), & \text{if } \sqrt{x^2 + y^2} < 10, \\ (1, 0, 0, 1, 1), & \text{otherwise}, \end{cases}$$

where $\tan\theta = y/x$ and use the following parameters:

$$\gamma = 1.2, \quad q_0 = 50, \quad \frac{1}{\varepsilon} = 1000, \quad \tau_c = 3.$$

We take the computational domain $[-30, 100] \times [-30, 30]$, on which we implement free boundary conditions, and use a uniform spatial mesh with $\Delta x = \Delta y = 0.5$. The results (density, temperature, and fraction of unburnt gas) obtained by the ADP and SDP methods at times $t = 0.25, 1, 3, 4, 5$ are reported in Figures 4.6–4.8. As one can observe, both methods provide similar approximations at small times $t = 0.25$ and 1 (before the collision). At a later time $t = 3$ (after the collision with the shock, but before the collision with the rarefaction wave), the densities
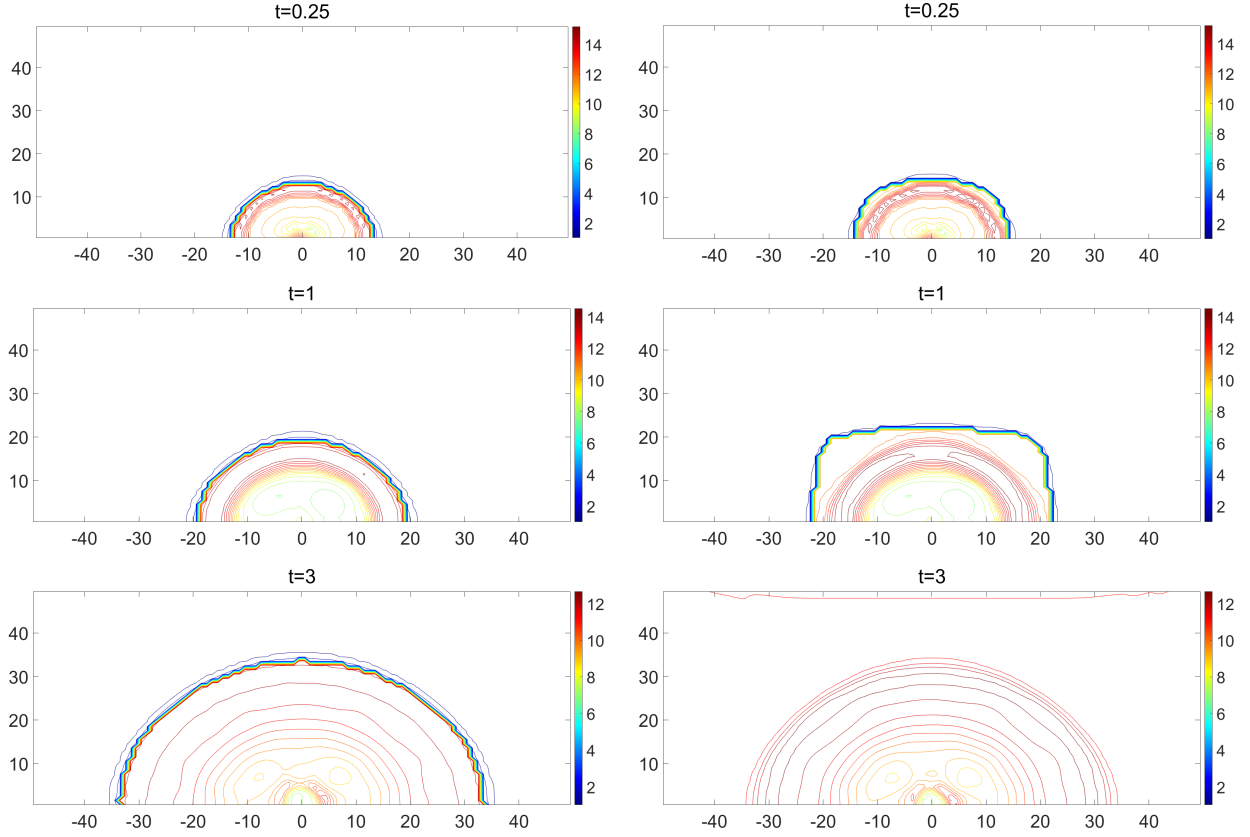
Figure 4.4: Example 2: Temperature τ computed by the ADP (left column) and SDP (right column) methods.

computed by the ADP and SDP methods still look similar while the temperatures start exhibiting a different behavior. The latter is due to the fact that, similarly to the 1-D case studied in [19], the detonation wave produced by the SDP method starts moving with an unphysical speed. Finally, at times $t = 4$ and 5 (after all the collisions), the detonation wave front computed by the SDP method keeps moving to the right with the increasing non-physical speed. At the same time, the ADP method seems to produce accurate results.

Example 4—Diffraction of a Detonation Wave

In the final example, we consider a detonation wave in the domain $[-1, 0] \times [0, 1] \cup [0, 3] \times [-1, 1]$ with the solid walls along the top part of the boundary and along the following line segments: $\{-1 \le x \le 0,\ y = 0\}$, $\{x = 0,\ -1 \le y \le 0\}$, and $\{0 \le x \le 3,\ y = -1\}$, and the open boundaries on the left and on the right. The initial data are

$$(\rho, u, v, p, z)(x, y, 0) = \begin{cases} (3.64282, 6.2489, 0, 54.8244, 0), & \text{if } x \le -0.5, \\ (1, 0, 0, 1, 1), & \text{if } x > -0.5, \end{cases}$$

and the parameters are the same as in Example 2:

$$\gamma = 1.2, \quad q_0 = 50, \quad \frac{1}{\varepsilon} = 1000, \quad \tau_c = 2.$$
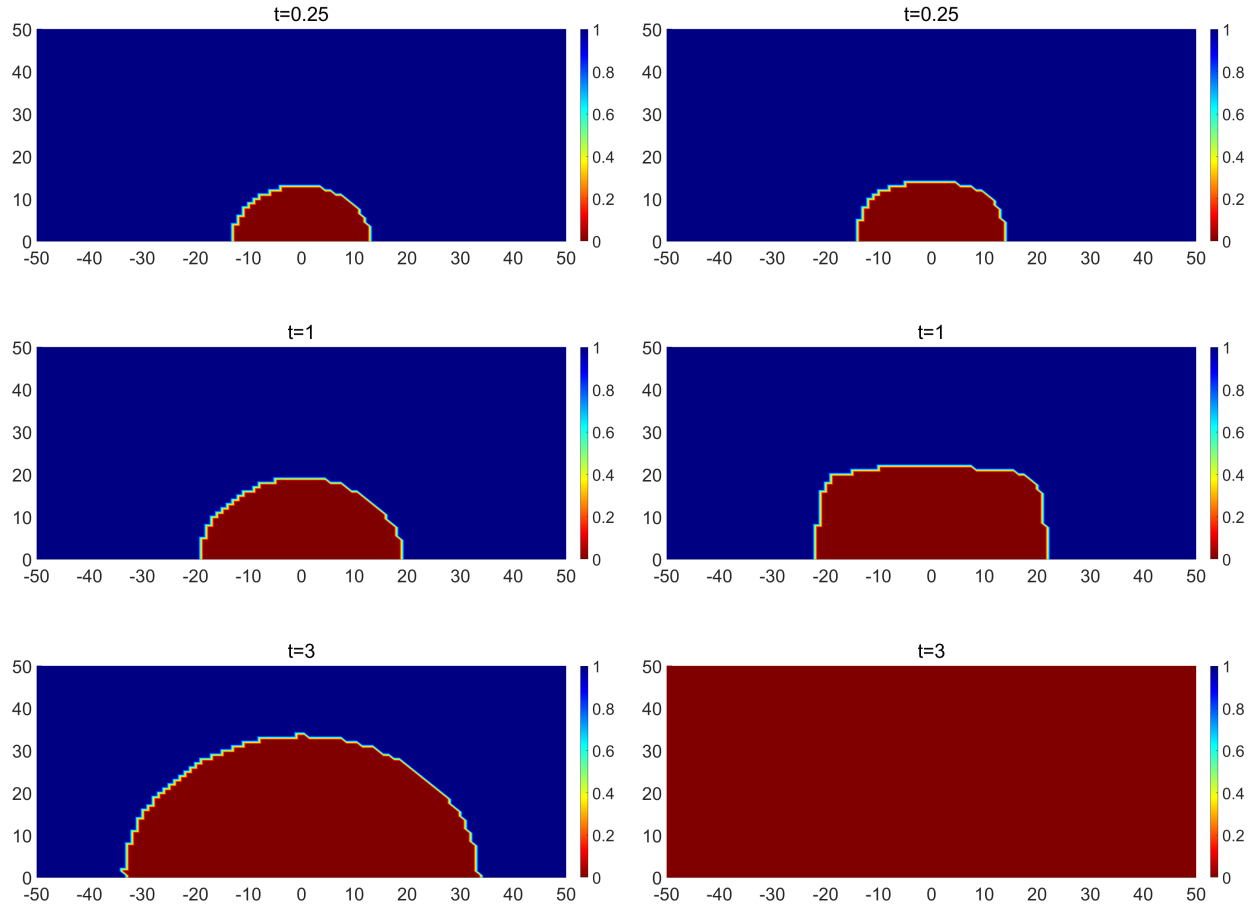
Figure 4.5: Example 2: Fraction of unburned gas z (shaded in red) computed by the ADP (left column) and SDP (right column) methods.

The initial setting is outlined in Figure 4.10.

In this example, the detonation wave initially positioned vertically at $x = -0.5$, first propagates to the right and then diffracts around a solid corner. We compute the solution at times $t = 0.2$ and 0.4 on a uniform spatial grid with $\Delta x = \Delta y = 1/100$ using both the ADP and SDP methods. The results are shown in Figures 4.10 and 4.11, where we plot the density, temperature and the fraction of unburnt gas fields. As one can clearly see, an artificially fast wave generated by the SDP method after the diffraction, is prevented by the use of the proposed ADP procedure.

5   Conclusion

In this paper, we have considered inviscid, compressible, reactive flows governed by the Euler equations coupled with a transport equation for the fraction of unburnt gas. For small reaction times, the chemical reaction may be considered infinitely fast and thus the transport equation has a stiff source term, which can be efficiently treated by projecting the computed solution onto an equilibrium state. A straightforward projection however has a major drawback: it may lead to a spurious detonation wave that travels with an unphysical speed even if the scheme is stable, as we illustrated in our numerical examples. Here, we have shown how the "standard" deterministic
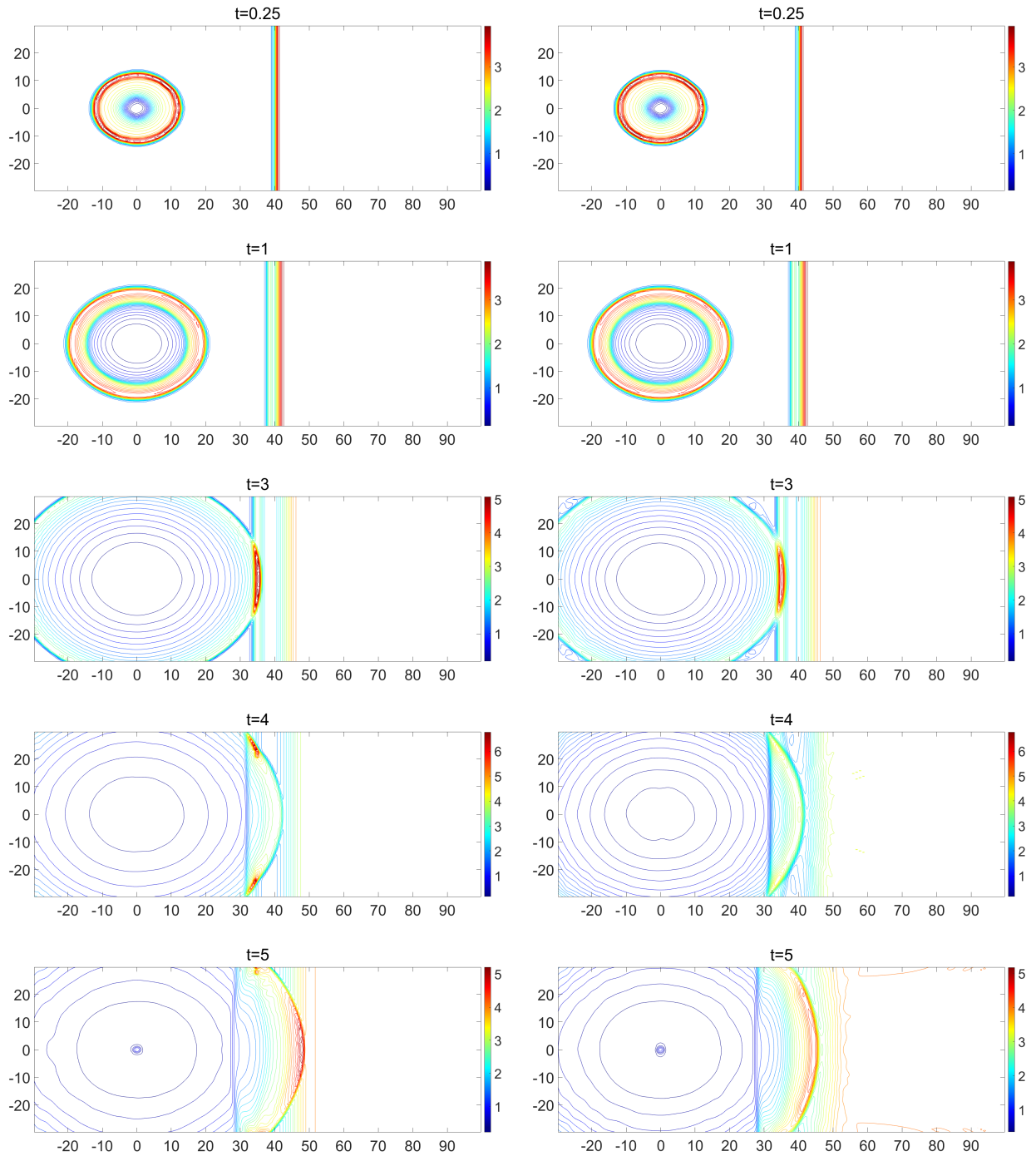
Figure 4.6: Example 3: Density ρ computed by the ADP (left column) and SDP (right column) methods.

projection approach can be modified to provide an accurate approximation for the underlying model. As the result, we have designed a simple, robust and stable underresolved method for stiff detonation waves using an accurate deterministic projection (ADP) approach and demonstrated that the proposed computational technique guarantees that the detonation waves will propagate with a physically relevant speed.
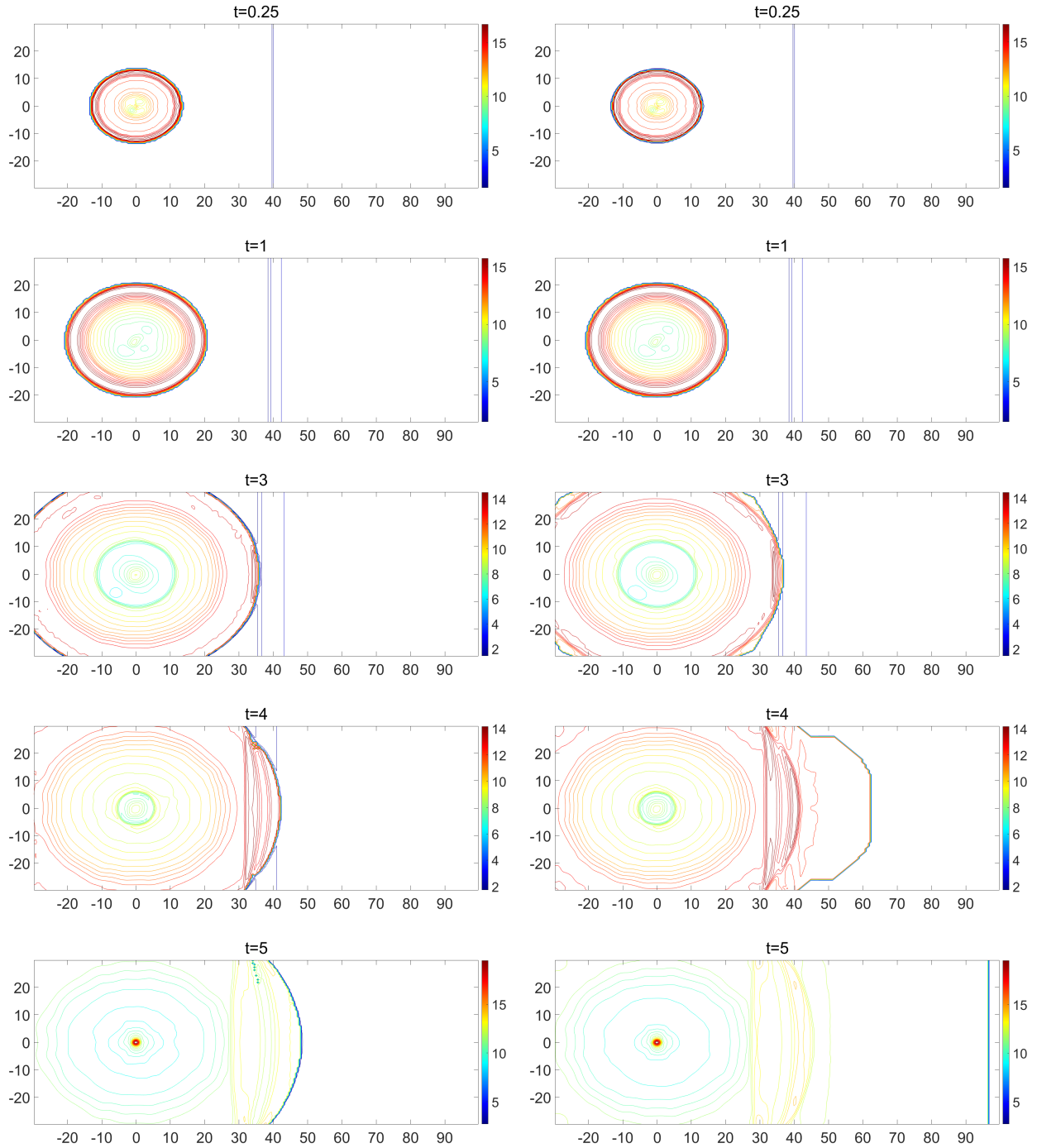
Figure 4.7: Example 3: Temperature τ computed by the ADP (left column) and SDP (right column) methods.

We believe that the proposed ADP method, though developed for the case of stiff detonation waves, may also be applicable to less stiff Chapman-Jouguet detonation waves. It can also extended to multi-species reactive Euler equations. We leave these investigations for the future work.
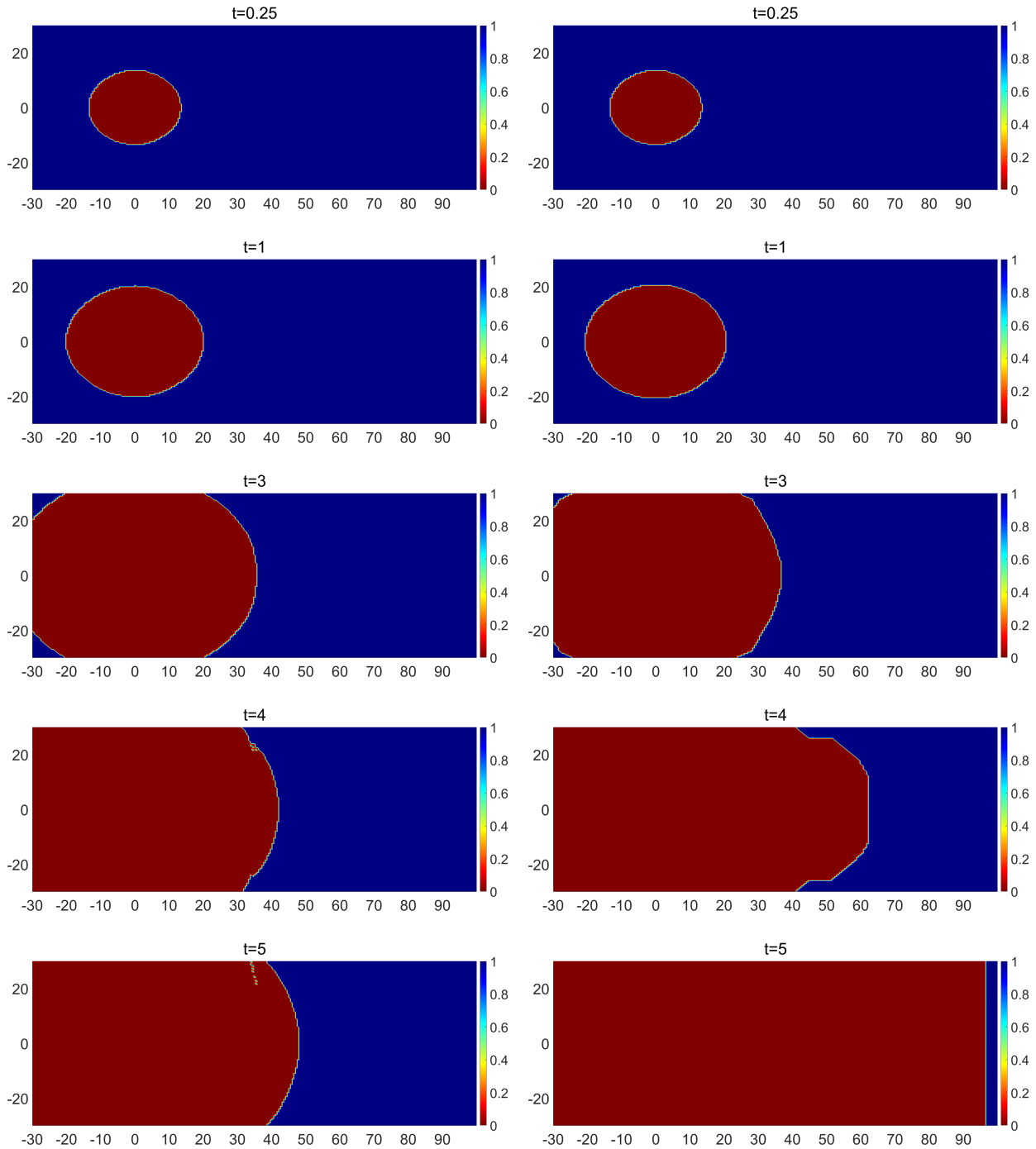
Figure 4.8: Example 3: Fraction of unburned gas z (shaded in red) computed by the ADP (left column) and SDP (right column) methods.
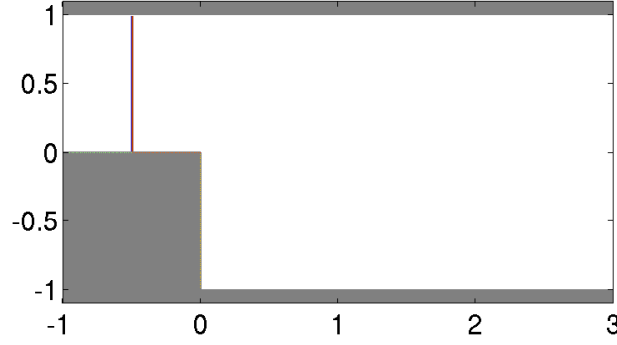
Figure 4.9: Example 4: Domain and the initial wave location.

A   Semi-Discrete Central-Upwind Scheme

In this section, we briefly describe the semi-discrete central-upwind scheme for the homogeneous 2-D systems (2.1), (1.3) and (3.1), (1.3). The 2-D semi-discrete central-upwind scheme from [24] admits the following flux form:

$$\frac{d}{dt}\overline{\boldsymbol{U}}_{j,k}(t) = -\frac{\boldsymbol{H}^x_{j+\frac{1}{2},k} - \boldsymbol{H}^x_{j-\frac{1}{2},k}}{\Delta x} - \frac{\boldsymbol{H}^y_{j,k+\frac{1}{2}} - \boldsymbol{H}^y_{j,k-\frac{1}{2}}}{\Delta y}, \tag{A.1}$$

where the numerical fluxes are

$$
\begin{aligned}
\boldsymbol{H}^x_{j+\frac{1}{2},k} &= \frac{a^+_{j+\frac{1}{2},k}\boldsymbol{F}(\boldsymbol{U}^{\mathrm{E}}_{j,k}) - a^-_{j+\frac{1}{2},k}\boldsymbol{F}(\boldsymbol{U}^{\mathrm{W}}_{j+1,k})}{a^+_{j+\frac{1}{2},k} - a^-_{j+\frac{1}{2},k}} + \frac{a^+_{j+\frac{1}{2},k}a^-_{j+\frac{1}{2},k}}{a^+_{j+\frac{1}{2},k} - a^-_{j+\frac{1}{2},k}}\left[\boldsymbol{U}^{\mathrm{W}}_{j+1,k} - \boldsymbol{U}^{\mathrm{E}}_{j,k}\right], \\
\boldsymbol{H}^y_{j,k+\frac{1}{2}} &= \frac{b^+_{j,k+\frac{1}{2}}\boldsymbol{G}(\boldsymbol{U}^{\mathrm{N}}_{j,k}) - b^-_{j,k+\frac{1}{2}}\boldsymbol{G}(\boldsymbol{U}^{\mathrm{S}}_{j,k+1})}{b^+_{j,k+\frac{1}{2}} - b^-_{j,k+\frac{1}{2}}} + \frac{b^+_{j,k+\frac{1}{2}}b^-_{j,k+\frac{1}{2}}}{b^+_{j,k+\frac{1}{2}} - b^-_{j,k+\frac{1}{2}}}\left[\boldsymbol{U}^{\mathrm{N}}_{j,k+1} - \boldsymbol{U}^{\mathrm{S}}_{j,k}\right].
\end{aligned}
\tag{A.2}
$$

The quantities $\overline{\boldsymbol{U}}_{j,k}$, $\boldsymbol{H}^x_{j,k}$, $\boldsymbol{H}^y_{j,k}$, $a^+_{j,k}$, $a^-_{j,k}$, $\boldsymbol{U}^{\mathrm{E}}_{j,k}$, $\boldsymbol{U}^{\mathrm{W}}_{j,k}$, $\boldsymbol{U}^{\mathrm{N}}_{j,k}$ and $\boldsymbol{U}^{\mathrm{S}}_{j,k}$ depend in fact on t, but we suppress this dependence for the sake of brevity.

In (A.2),

$$
\boldsymbol{U}^{\mathrm{E}}_{j,k} = \overline{\boldsymbol{U}}_{j,k} + \frac{\Delta x}{2}(\boldsymbol{U}_x)_{j+\frac{1}{2},k}, \qquad \boldsymbol{U}^{\mathrm{W}}_{j,k} = \overline{\boldsymbol{U}}_{j,k} - \frac{\Delta x}{2}(\boldsymbol{U}_x)_{j+\frac{1}{2},k},
$$

$$
\boldsymbol{U}^{\mathrm{N}}_{j,k} = \overline{\boldsymbol{U}}_{j,k} + \frac{\Delta y}{2}(\boldsymbol{U}_y)_{j,k+\frac{1}{2}}, \qquad \boldsymbol{U}^{\mathrm{S}}_{j,k} = \overline{\boldsymbol{U}}_{j,k} - \frac{\Delta y}{2}(\boldsymbol{U}_y)_{j,k+\frac{1}{2}}
$$

are the point values of the piecewise linear reconstruction

$$\widetilde{\boldsymbol{U}}(x,y) = \overline{\boldsymbol{U}}_{j,k} + (\boldsymbol{U}_x)_{j,k}(x - x_j) + (\boldsymbol{U}_y)_{j,k}(y - y_k) \quad \text{for } (x,y) \in \left(x_{j-\frac{1}{2}}, x_{j+\frac{1}{2}}\right) \times \left(y_{k-\frac{1}{2}}, y_{k+\frac{1}{2}}\right)$$

at the midpoints of the edges of cell (j,k).
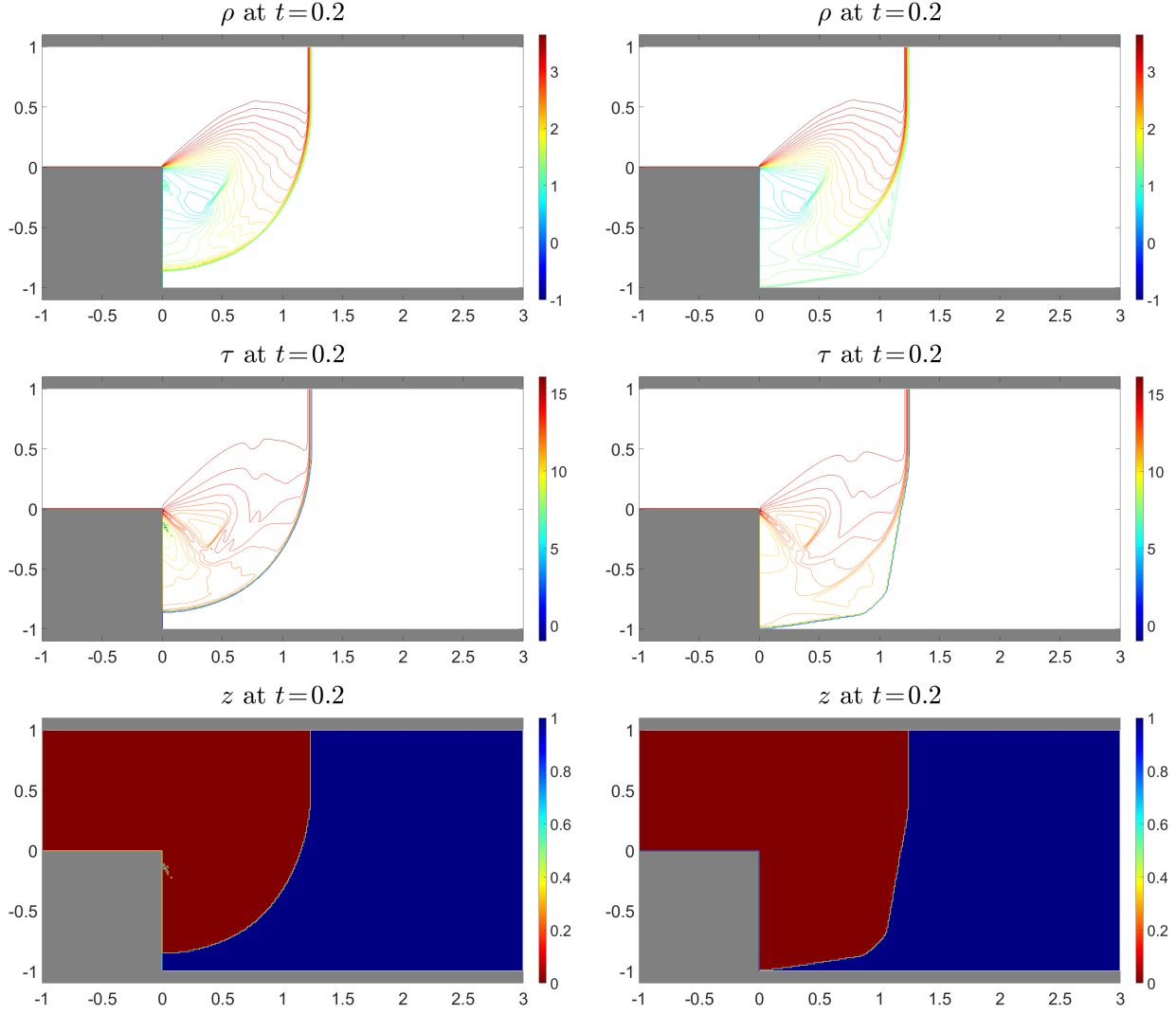
Figure 4.10: Example 4: Density ρ (top row), temperature τ (middle row) and the fraction of unburnt gas z (bottom row) at time $t = 0.2$ computed by the ADP (left column) and SDP (right column) methods.

The numerical derivatives $(\boldsymbol{U}_x)_{j,k}$ and $(\boldsymbol{U}_y)_{j,k}$ are to be computed using a nonlinear limiter. We have used a minmod limiter (see, e.g., [28, 30, 31]), which gives

$$(\boldsymbol{U}_x)_{j,k} = \text{minmod}\left(\frac{\overline{\boldsymbol{U}}_{j+1,k} - \overline{\boldsymbol{U}}_{j,k}}{\Delta x}, \ \frac{\overline{\boldsymbol{U}}_{j,k} - \overline{\boldsymbol{U}}_{j-1,k}}{\Delta x}\right),$$

$$(\boldsymbol{U}_y)_{j,k} = \text{minmod}\left(\frac{\overline{\boldsymbol{U}}_{j,k+1} - \overline{\boldsymbol{U}}_{j,k}}{\Delta y}, \ \frac{\overline{\boldsymbol{U}}_{j,k} - \overline{\boldsymbol{U}}_{j,k-1}}{\Delta y}\right),$$

where the minmod function is defined as

$$\text{minmod}(a, b) := \frac{\text{sgn}(a) + \text{sgn}(b)}{2} \cdot \min(|a|, |b|).$$

One-sided local propagation speeds in the x- and y-directions $a^{\pm}_{j+\frac{1}{2},k}$ and $b^{\pm}_{j,k+\frac{1}{2}}$ are obtained using the largest/smallest eigenvalues of the Jacobian. For the reactive Euler systems (2.1), (1.3)
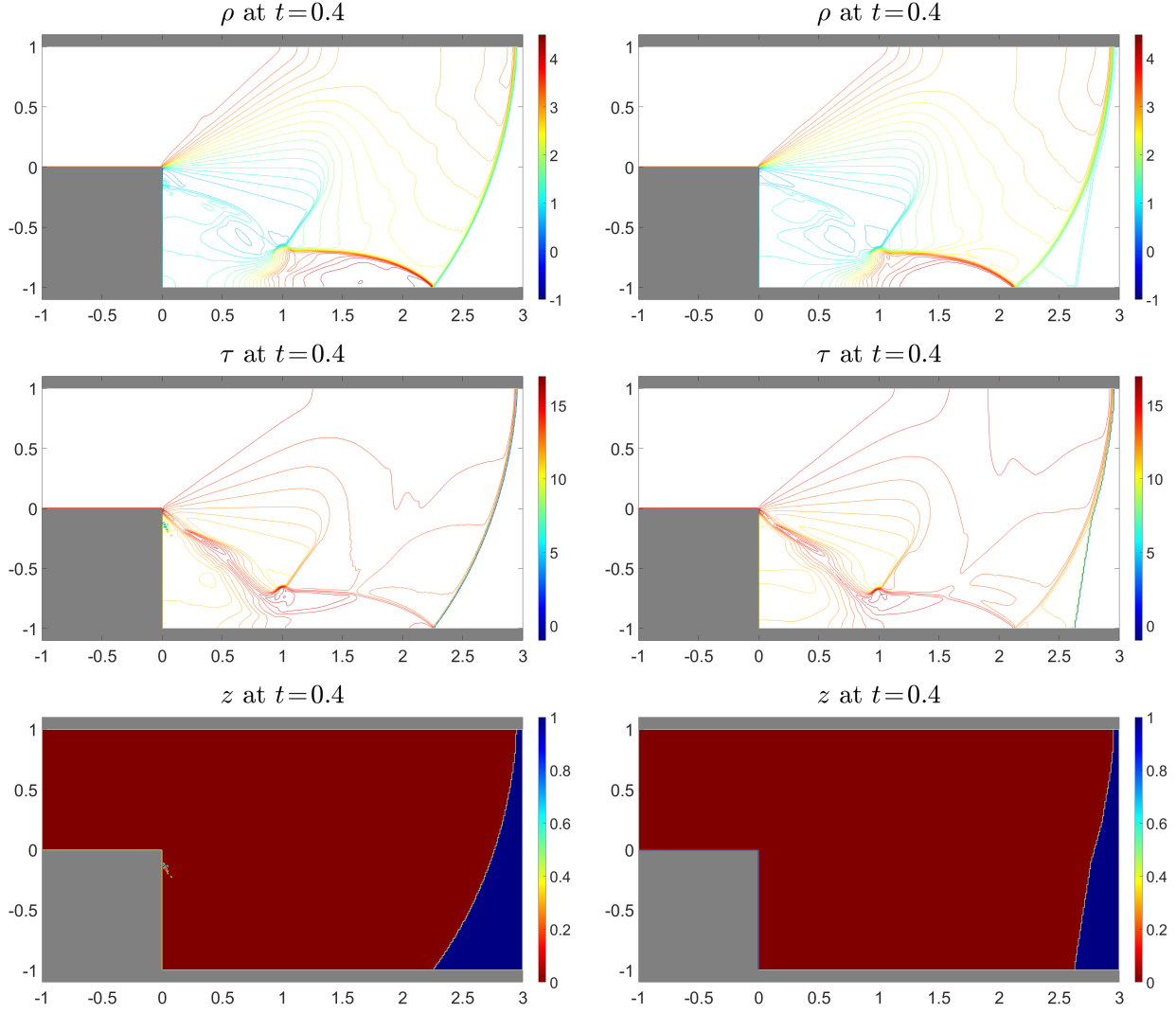
Figure 4.11: Example 4: Same as in Figure 4.8, but at time $t = 0.4$.

and (3.1), (1.3), we obtain

$$a_{j+\frac{1}{2},k}^{+} = \max\left(u_{j,k}^{\mathrm{E}} + \sqrt{\frac{\gamma p_{j,k}^{\mathrm{E}}}{\rho_{j,k}^{\mathrm{E}}}},\ u_{j+1,k}^{\mathrm{W}} + \sqrt{\frac{\gamma p_{j+1,k}^{\mathrm{W}}}{\rho_{j,k}^{\mathrm{W}}}},\ 0\right),$$

$$a_{j+\frac{1}{2},k}^{-} = \min\left(u_{j,k}^{\mathrm{E}} - \sqrt{\frac{\gamma p_{j,k}^{\mathrm{E}}}{\rho_{j,k}^{\mathrm{E}}}},\ u_{j+1,k}^{\mathrm{W}} - \sqrt{\frac{\gamma p_{j+1,k}^{\mathrm{W}}}{\rho_{j,k}^{\mathrm{W}}}},\ 0\right),$$

$$b_{j,k+\frac{1}{2}}^{+} = \max\left(u_{j,k}^{\mathrm{N}} + \sqrt{\frac{\gamma p_{j,k}^{\mathrm{N}}}{\rho_{j,k}^{\mathrm{N}}}},\ u_{j,k+1}^{\mathrm{S}} + \sqrt{\frac{\gamma p_{j,k+1}^{\mathrm{S}}}{\rho_{j,k}^{\mathrm{S}}}},\ 0\right),$$

$$b_{j,k+\frac{1}{2}}^{-} = \min\left(u_{j,k}^{\mathrm{N}} - \sqrt{\frac{\gamma p_{j,k}^{\mathrm{N}}}{\rho_{j,k}^{\mathrm{N}}}},\ u_{j,k+1}^{\mathrm{S}} - \sqrt{\frac{\gamma p_{j,k+1}^{\mathrm{S}}}{\rho_{j,k}^{\mathrm{S}}}},\ 0\right).$$

Finally, the ODE system (A.1) is numerically integrated by the three-stage third-order strong

stability preserving (SSP) Runge-Kutta method; see, [12, 13].

References

[1] W. Bao and S. Jin, *The random projection method for hyperbolic conservation laws with stiff reaction terms*, J. Comput. Phys., 163 (2000), pp. 216–248.

[2] W. Bao and S. Jin, *The random projection method for stiff detonation capturing*, SIAM J. Sci. Comput., 23 (2001), pp. 1000–1026 (electronic).

[3] M. Ben-Artzi, *The generalized Riemann problem for reactive flows*, J. Comput. Phys., 81 (1989), pp. 70–101.

[4] A. C. Berkenbosch, *Capturing detonation waves for the reactive Euler equations*, PhD thesis, Department of Mathematics and Computer Science, Technische Universiteit Eindhoven, 1995.

[5] A. C. Berkenbosch, E. F. Kaasschieter, and R. Klein, *Detonation capturing for stiff combustion chemistry*, Combust. Theory Model., 2 (1998), pp. 313–348.

[6] A. Bourlioux, A. J. Majda, and V. Roytburd, *Theoretical and numerical structure for unstable one-dimensional detonations*, SIAM J. Appl. Math., 51 (1991), pp. 303–343.

[7] A. Chertock and A. Kurganov, *On a practical implementation of particle methods*, Appl. Numer. Math., 56 (2006), pp. 1418–1431.

[8] A. J. Chorin, *Random choice methods with applications to reacting gas flow*, J. Comput. Phys., 25 (1977), pp. 253–272.

[9] P. Colella, A. Majda, and V. Roytburd, *Fractional step methods for reacting shock waves*, in Reacting flows: combustion and chemical reactors, Part 2 (Ithaca, N.Y., 1985), vol. 24 of Lectures in Appl. Math., Amer. Math. Soc., Providence, RI, 1986, pp. 459–477.

[10] P. Colella, A. Majda, and V. Roytburd, *Theoretical and numerical structure for reacting shock waves*, SIAM J. Sci. Statist. Comput., 7 (1986), pp. 1059–1080.

[11] R. P. Fedkiw, T. Aslam, and S. Xu, *The ghost fluid method for deflagration and detonation discontinuities*, J. Comput. Phys., 154 (1999), pp. 393–427.

[12] S. Gottlieb, D. Ketcheson, and C.-W. Shu, *Strong stability preserving Runge-Kutta and multistep time discretizations*, World Scientific Publishing Co. Pte. Ltd., Hackensack, NJ, 2011.

[13] S. Gottlieb, C.-W. Shu, and E. Tadmor, *Strong stability-preserving high-order time discretization methods*, SIAM Rev., 43 (2001), pp. 89–112.

[14] D. F. Griffiths, A. M. Stuart, and H. C. Yee, *Numerical wave propagation in an advection equation with a nonlinear source term*, SIAM J. Numer. Anal., 29 (1992), pp. 1244–1260.

[15] C. Helzel, R. J. Leveque, and G. Warnecke, *A modified fractional step method for the accurate approximation of detonation waves*, SIAM J. Sci. Comput., 22 (2000), pp. 1489–1510.

[16] W. D. Henshaw and D. W. Schwendeman, *An adaptive numerical scheme for high-speed reactive flow on overlapping grids*, J. Comput. Phys., 191 (2003), pp. 420–447.

[17] W. D. Henshaw and D. W. Schwendeman, *Moving overlapping grids with adaptive mesh refinement for high-speed reactive and non-reactive flow*, J. Comput. Phys., 216 (2006), pp. 744–779.

[18] P. Hwang, R. Fedkiw, B. Merriman, T. Aslam, A. Karagozian, and S. Osher, *Numerical resolution of pulsating detonation waves*, Combust. Theory Modelling, 4 (2000), pp. 217–240.

[19] A. Kurganov, *An accurate deterministic projection method for hyperbolic systems with stiff source term*, in Hyperbolic problems: theory, numerics, applications, Springer, Berlin, 2003, pp. 665–674.

[20] A. Kurganov and C.-T. Lin, *On the reduction of numerical dissipation in central-upwind schemes*, Commun. Comput. Phys., 2 (2007), pp. 141–163.

[21] A. Kurganov, S. Noelle, and G. Petrova, *Semidiscrete central-upwind schemes for hyperbolic conservation laws and Hamilton-Jacobi equations*, SIAM J. Sci. Comput., 23 (2001), pp. 707–740.

[22] A. Kurganov, M. Prugger, and T. Wu, *Second-order fully discrete central-upwind scheme for two-dimensional hyperbolic systems of conservation laws*, SIAM J. Sci. Comput., 39 (2017), pp. A947–A965.

[23] A. Kurganov and E. Tadmor, *New high-resolution central schemes for nonlinear conservation laws and convection-diffusion equations*, J. Comput. Phys., 160 (2000), pp. 241–282.

[24] A. Kurganov and E. Tadmor, *Solution of two-dimensional Riemann problems for gas dynamics without Riemann problem solvers*, Numer. Methods Partial Differential Equations, 18 (2002), pp. 584–608.

[25] R. J. LeVeque and H. C. Yee, *A study of numerical methods for hyperbolic conservation laws with stiff source terms*, J. Comput. Phys., 86 (1990), pp. 187–210.

[26] M.-S. Liou, *A sequel to AUSM: AUSM$^+$*, J. Comput. Phys., 129 (1996), pp. 364–382.

[27] M.-S. Liou and C. J. Steffen, Jr., *A new flux splitting scheme*, J. Comput. Phys., 107 (1993), pp. 23–39.

[28] H. Nessyahu and E. Tadmor, *Nonoscillatory central differencing for hyperbolic conservation laws*, J. Comput. Phys., 87 (1990), pp. 408–463.

[29] R. B. Pember, *Numerical methods for hyperbolic conservation laws with stiff relaxation. I. Spurious solutions*, SIAM J. Appl. Math., 53 (1993), pp. 1293–1330.

[30] P. K. Sweby, *High resolution schemes using flux limiters for hyperbolic conservation laws*, SIAM J. Numer. Anal., 21 (1984), pp. 995–1011.

[31] B. van Leer, *Towards the ultimate conservative difference scheme. V. A second-order sequel to Godunov's method*, J. Comput. Phys., 32 (1979), pp. 101–136.

[32] W. Wang, C.-W. Shu, H. C. Yee, and B. Sjögreen, *High order finite difference methods with subcell resolution for advection equations with stiff source terms*, J. Comput. Phys., 231 (2012), pp. 190–214.

[33] F. A. Williams, *Combustion Theory*, Addison-Wesley, Reading, MA, 1965.

[34] B. Yu, L. Li, B. Zhang, and J. Wang, *An approach to obtain the correct shock speed for Euler equations with stiff detonation*, Commun. Comput. Phys., 22 (2017), pp. 259–284.